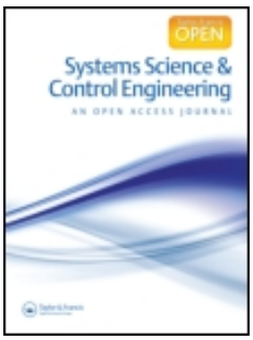

Systems Science & Control Engineering: An Open Access Journal

ISSN: (Print) 2164-2583 (Online) Journal homepage: http://www.tandfonline.com/loi/tssc20

# Design and implementation of an open circuit voltage prediction mechanism for lithium-ion battery systems

T. Stockley, K. Thanapalan, M. Bowkett & J. Williams

**To cite this article:** T. Stockley, K. Thanapalan, M. Bowkett & J. Williams (2014) Design and implementation of an open circuit voltage prediction mechanism for lithium-ion battery systems, Systems Science & Control Engineering: An Open Access Journal, 2:1, 707-717, DOI: 10.1080/21642583.2014.956268

**To link to this article:** https://doi.org/10.1080/21642583.2014.956268



Accepted author version posted online: 15 Sep 2014.
Published online: 22 Sep 2014.

*Systems Science & Control Engineering: An Open Access Journal*, 2014
Vol. 2, 707–717, http://dx.doi.org/10.1080/21642583.2014.956268

Taylor & Francis
Taylor & Francis Group

# Design and implementation of an open circuit voltage prediction mechanism for lithium-ion battery systems

T. Stockley*, K. Thanapalan, M. Bowkett and J. Williams

*Centre for Automotive & Power System Engineering (CAPSE), Faculty of Computing, Engineering and Science, University of South Wales, Treforest, UK*

(*Received 31 January 2014; final version received 16 August 2014*)

This paper describes an open circuit voltage (OCV) prediction technique for lithium cells. The work contains an investigation to examine the charge and mixed state relaxation voltage curves, to analyse the potential for the OCV prediction technique in a practical system. The underlying principal of the technique described in this paper employs a simple equation paired with a polynomial to predict the equilibrated cell voltage after a small rest period. The polynomial coefficients are devised by the use of curve fitting and system identification techniques. The practical work detailed in this paper was conducted at the Centre for Automotive and Power System Engineering (CAPSE) battery laboratories at the University of South Wales. The results indicate that the proposed OCV prediction technique is highly effective and may be implemented with a simple battery management system.

**Keywords:** OCV; cell relaxation; lithium technology; battery system performance; prediction mechanism

## 1. Introduction

This paper investigates the effect of a constant current charge and mixed state duty cycle, and how the cell voltage reacts when in a state of suspension. Previous research work relating to this study proved that a simple equation is adequate for an improved accuracy open circuit voltage (OCV) measurement. The study also provided a detailed explanation of how constant current discharges affect such lithium cell OCV measurements (Stockley, Thanapalan, Bowkett, & Williams, 2013).

The reliance that the world's consumer markets have placed on battery technologies can be seen in the vast amount of applications required today. Typically used in portable electronic devices such as cell phones and small items of equipment (Zhang & Harb, 2013), lithium battery technologies are now becoming more common in the automotive sector (Weinert, Burke, & Wei, 2007) in its quest to power the next generation of clean, green vehicles (Affanni, Bellini, Franceschini, Guglielmi, & Tassoni, 2005). A less obvious application is their integration into many stationary applications. The industrial applications include backup power systems for the telecommunications industry (Lu, Han, Li, Hua, & Ouyang, 2013; Suzuki, Shizuki, & Nishiyama, 2003), and energy storage for renewable energy systems (Li et al., 2012).

There are several large battery technologies being used in today's industry. The following advantages are gained through using lithium technologies over other cell chemistries: (i) a higher cell voltage, which is key to the high energy density; (ii) greatly improved cycle count, with typical figures of 300–400 cycles; (iii) a more consistent manufacturing process between cells of the same type, resulting in more balanced battery modules and (iv) an improved specific energy and energy density. However, the benefits of lithium batteries are counterbalanced by several drawbacks: (i) high initial cost – although prices are reducing with increased high volume production; (ii) costly electronics for the battery management system (BMS) to protect the cells; (iii) increased risk of overheating and fire due to the high energy, albeit this is mitigated by the use of a BMS and safer cell chemistries. Failure to implement a BMS or the consequences of error can result in overheating, fire or explosion such as the well-publicised incidents in 2006 (Sima, 2006).

The function of the BMS extends beyond preventing damage to the lithium cells. BMSs also contribute to the advantages of using the lithium technology. The BMS monitors the voltage level of each of the cells in the battery pack to ensure that the cells are well balanced, which increases the performance of the battery pack (Bowkett, Thanapalan, Stockley, Hathway, & Williams, 2013). A key element of the BMS is estimation of the state of charge (SoC) of the battery. The SoC indicates what percentage of the battery capacity has been used so that the user can recharge the cells when necessary. The most common SoC estimation techniques are referred to as follows.

*Corresponding author. Email: thomas.stockley@southwales.ac.uk

Coulomb counting is the most basic capacity measurement technique and is typically implemented in the majority of BMSs available to date. The method works by counting the Amp-hours (Ah) in and out of a cell/battery and then calculating how many Ah are left as a percentage of the initial capacity (Ng, Moo, Chen, & Hsieh, 2009). Although extremely simple to implement and requiring very little processing space and time, this method does have two major disadvantages: (i) the initial SoC of the cell/battery must be known or calculation errors occur and (ii) the capacity of the cell must be known, and this value changes with both temperature and age.

A spectrum of frequencies is used by electrochemical impedance spectroscopy (EIS) methods to measure the internal resistance and the impedance of the cell. By measuring these factors, the SoC of the cell can be obtained as (Salkind, Fennie, Singh, Atwater, & Reisner, 1999) has for NiMH cells. Whilst this method is very accurate, the cell must be fully equilibrated, requiring an unused state of between 2 and 6 hours for lithium cells prior to measurement. It is, therefore, impractical for real-time use in many applications.

The OCV of a cell can be used to find the SoC of the cell due to its relationship (Chiang, Sean, & Ke, 2011). This method can accurately estimate the SoC; however, research indicates that the OCV is temperature reliant (Pop et al., 2006). It has been shown by Roscher and Sauer (2011) that OCV is prevented from being the same after a charge and discharge for the same SoC by hysteresis. The introduction of a recovery factor to decide whether the cell has performed a charge or discharge has reduced the error in OCV–SoC measurements (Roscher & Sauer, 2011). As with the EIS method, a long rest period is required because the cell needs to be equilibrated for an accurate measurement to be taken. Work has been completed by Aylor, Thieme, and Johnson (1992) on an OCV prediction technique which estimates what the OCV will be after 3 hours, from a single measurement taken at 30 minutes, allowing the OCV–SoC method to be used practically.

Aylor et al. (1992) provided two methods of OCV prediction for lead acid batteries. The techniques estimate what the OCV will be after 3 hours, from a single measurement taken at 30 minutes, allowing the OCV–SoC method to be used practically. In their work two methods are identified: (i) a simple summing method is used to quickly calculate the SoC of the battery. This method was disregarded due to the varying performance of lead acid batteries even from the same production batch. The simple summing method provided disappointing results for Aylor et al. when used on lead acid batteries. However, Stockley et al. (2013) showed very promising results when the summing method was applied to two different chemistry-based lithium ion cells. (ii) A more complex method is provided to eliminate the problems encountered in the first method. This method uses asymptotes on a logarithmic scale and proves viable with errors in SoC estimation of less than 5% and a prediction time of just 6.6 minutes.

The asymptote method has been proven to work on lithium cells as well as lead acid batteries (Pop, Bergveld, Danilov, Regiten, & Notten, 2008). This method was used to validate the model proposed by Pop et al. (2008), but in doing so was effectively utilised when adapted to lithium cells. Three different methods were used throughout the paper, with the asymptote method giving an error of just 0.92% SoC, an improvement from the 20.19% SoC provided by a combination of a voltage change model and a temperature model. However, the asymptote method was trumped in accuracy by the model developed by Pop et al., which works on the voltage relaxation accounting for temperature, SoC, charge/discharge rate and age of the cell. The accuracy of the model by Pop et al. achieved an error of 0.19% SoC.

The work conducted by Weng, Sun, and Peng (2013) uses a new sigmoid function approach to provide a model capable of predicting the OCV of a lithium cell. The author compared the proposed model to several polynomial based models to good effect with an error of 2.5, 4.8 mV lower than the most accurate polynomial model. The SoC comparison and also SoH comparison are proven to be effective when combined with an extended Kalman filter (EKF).

Pei, Wang, Lu, and Zhu (2014) uses a combination of practical tests on a lithium iron phosphate cell and a theoretical second-order resistor capacitor equivalent circuit to show that the long relaxation time is due to the diffusion process. The diffusion process was then proven to have a linear relationship with the cell OCV. By using this information, a linear regression model has been created to determine the cell conditions before a voltage relaxation model can be used for the OCV prediction.

Polynomials have been used to reduce the relaxation time before OCV can be measured for both lithium iron phosphate and lithium manganese based cells in the work by Hu, Li, Peng, and Sun (2012). In their work the polynomials are used to model the curve of a lithium cell relaxation and then an EKF is used for the estimation of the SoC. This work paves the way for the work conducted in the remaining sections of this research work.

The remaining sections of this paper are as follows: Section 2 provides a brief explanation of the cell modelling and the simple equation used for the OCV prediction tests, and Section 3 explains how the tests were conducted. A summary of the background work is also presented in Section 3, followed by the constant current charge test results. Section 4 presents the mixed state relaxation test and implementation of the prediction mechanism. Section 4 also hosts a brief discussion of the polynomial which will allow rapid OCV prediction. Finally, a discussion of the results and the conclusions are presented at the end of the paper.

## 2. Modelling of a lithium cell

The OCV analysis carried out in the previous work has indicated that in order to obtain an accurate OCV measurement of a lithium cell, the cell needs to be in a fully equilibrated state. This is because the OCV is influenced by several factors, including cell chemistry, age of cell, cell temperature, charge/discharge rate and cell voltage characteristics. As has been previously mentioned, waiting for a cell to become equilibrated is a large disadvantage for the OCV–SoC estimation method because real world applications can rarely be halted for up to 3 hours for a measurement to be taken. Although several methods of OCV prediction were presented in the Introduction, it is thought that these methods are complicated and could prove too intense for simple BMS applications. Therefore, this work aims to develop a robust yet simple strategy to address the problems caused by the uncertainty that is associated with OCV prediction.

The proposed method comprises two sections: the first is to determine the OCV of the battery during relaxation, by using probabilistic methods such as what-if predictions. The second part is to determine the equilibrated OCV. Accurate prediction of OCV after a 30-minute relaxation period has been proven by Stockley et al. (2013), and will be incorporated in this work.

A mathematical model will be developed and incorporated to the original model developed by Stockley et al. (2013), resulting in a cascade-connected nonlinear model with a complex probabilistic component and a deterministic component.

Thus, the model will have the following form:

$$f = f_1 + f_2, \tag{1}$$

$$f_1 = \phi(t, \text{soc}, c, i), \tag{2}$$

where $\phi = \delta x^2 + \gamma x + \vartheta$, $\vartheta$ is the relaxation start voltage, and $\delta$ and $\gamma$ are the polynomial coefficients. The function $f_1$ is dependent upon the temperature ($t$), the SoC, the age of the cell ($c$) and the charge/discharge rate ($i$). All of the aforementioned parameters can be identified by monitoring the charge/discharge curve and by extrapolation of the battery voltage sampled during initial relaxation, or by the use of estimation algorithms. For example, Hu et al. (2012) used the linear regression model to predict the OCV. Function 1 is explored further in Section 4.

$$f_2 = V_{\text{tr}} \pm K_{\text{v}}, \tag{3}$$

where $V_{\text{tr}}$ is the voltage at a known measurement interval (8 minutes in this work, 30 minutes in Stockley et al. (2013)) and $K_{\text{v}}$ is a predefined constant derived from the equation $V_{\text{OC}} - V_{\text{tr}}$. Function 2 is the focus of this work and is found in Sections 3 and 4.

## 3. Measurement and monitoring

This section describes the test set-up, results and analysis of two types of lithium cell. It aims to prove that Equation (3) will be effective for both pouch and cylindrical lithium cells. The two types of cells that have been chosen for the tests in this section of work are the $LiNiMgCO_2 \cdot 20$ Ah pouch cell by Energy Innovation Group (EIG) and the $LiFePO_4 \cdot 8$ Ah cylindrical cell by Lifebatt.

### 3.1. *Experimental set-up*

To gain a greater knowledge of the relaxation curves of lithium cells, tests were conducted on two of the most common types of lithium cells, cylindrical and pouch type. Figures 1 and 2 show the pouch cell on test and a block diagram of the test set-up, respectively. As previously stated, the tests were conducted in the Centre for Automotive and Power System Engineering (CAPSE) laboratories at the University of South Wales. An industry standard cell tester unit was used to charge/discharge the cell with a temperature logger to monitor the ambient temperature.

### 3.2. *Similarity between cells*

For the implementation of the OCV prediction mechanism, the cells had to be proven to have a "clone-like" similarity between two cells of the same chemistry and type. To achieve this, tests were carried out (these were a 0.5C capacity test and a 0.3C relaxation test) which could be used to compare the two pouch cells. The cells used for these tests were $LiNiMgCO_2$ pouch cells. Figure 3 shows the results of the 0.5C capacity tests.

Figure 1. Testing of lithium pouch cell.

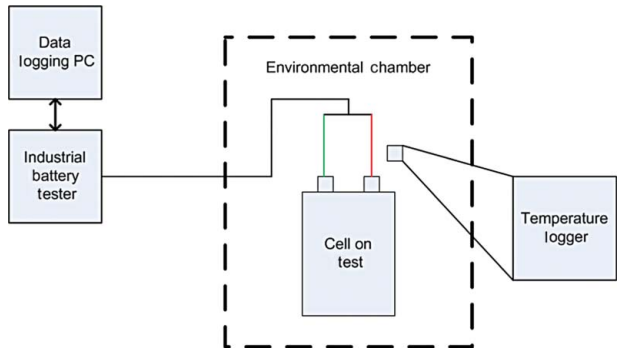


Figure 2. Block diagram of test equipment.

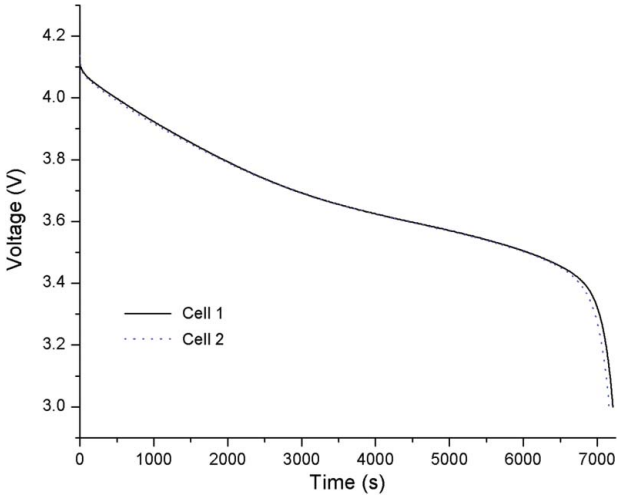


Figure 3. 0.5C discharge curves for pouch cell comparison.

As it can clearly be seen in Figure 3, the cells are almost a clone of each other throughout the discharge until the "knee" is reached. As Tremblay and Dessaint (2009) shows, the "knee" occurs during the final 20% of the discharge when the cell is placed under the most stress, and therefore, the cycle life is reduced. In Figure 4 the discharge voltage and the capacity of the cell are displayed, showing that the "knee" occurs within the last 10% SoC (less than 2 Ah). This means that even though there is a slight discrepancy between the two cells' data, use of the cell after this point should be avoided and, therefore, the results are largely irrelevant. Guena and Leblanc (2006) concur with Shim and Striebel (2003) and the concept that a cell's cycle life can be greatly improved by only using the cell within 70% of capacity.

Figure 5 shows a comparison of the relaxation voltages between the two $LiNiMgCO_2$ pouch cells to further highlight the clone-like effect. The relaxation tests were carried out at 80%, 60%, 40% and 20% SoC. This was so that a broad spectrum of results could be obtained that would represent the full capacity range of the cell. The relaxation curves were not measured at 0% SoC because the cells are rarely used below 20% SoC as mentioned earlier.

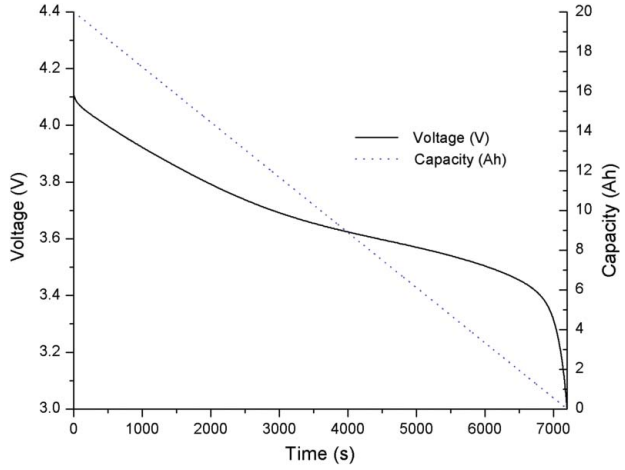


Figure 4. Cell capacity vs. voltage.

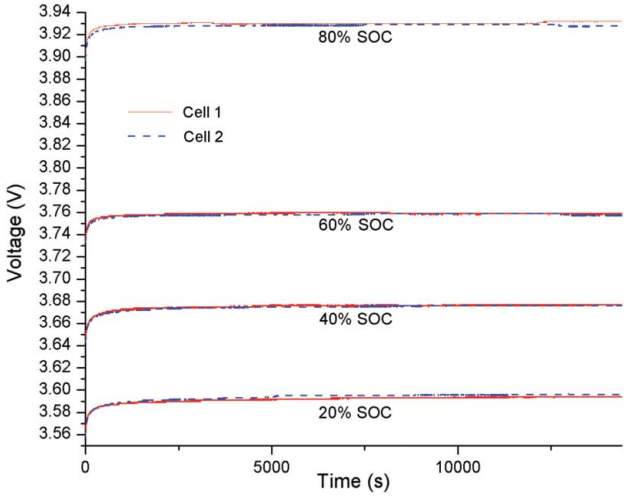


Figure 5. Relaxation curves following a 0.3C discharge for pouch cell comparison.

### 3.3. *Cell relaxation testing discharge state*

The cells' relaxation performance following a discharge state can be seen in Stockley et al. (2013), which also highlights the potential for an improved OCV prediction mechanism with very low prediction errors. This section presents a brief summary of the cell relaxation testing following a constant current discharge state.

The relaxation tests were conducted by discharging the cell at 20% SoC intervals, followed by a 4-hour open circuit period. The OCV was measured during the 4-hour rest period at a sample rate of 0.1 s to ensure the accuracy of the relaxation curves. The relaxation curves were measured at 80%, 60%, 40% and 20%, following a 0.3C, 1C and 3C discharge.

To ensure that the proposed OCV prediction technique was not limited to a particular type of cell, the tests were carried out on two types of cells. The two types of cells were not only two different package styles (pouch and

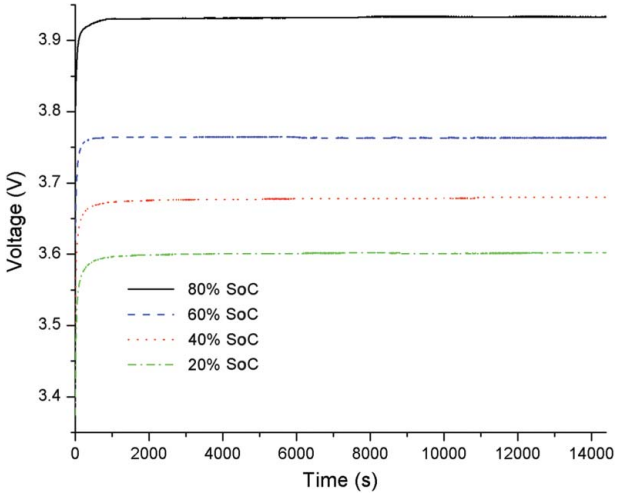


Figure 6. Relaxation curves of lithium pouch cell following a 1C discharge.

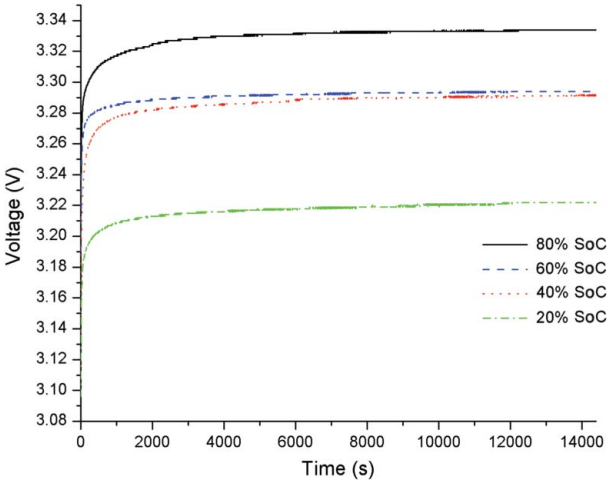


Figure 7. Relaxation curves of lithium cylindrical cell following a 1C discharge.

cylindrical), but also two different types of cell chemistries. The two different types of cell chemistries allowed the prediction technique to be conducted on different capacities and different operating voltages. Figures 6 and 7 show the discharge relaxation curves obtained for the pouch cell and the cylindrical cell, respectively.

The differences in the shape of the curves between Figures 6 and 7 were noted as being caused by the characteristic discharge curve from each type of cell. The difference in these discharge curves can be seen in Figure 8. As can be observed in Figure 8, the $LiNiMgCO_2$ cell has a very steep curve initially with a flat profile towards the end of discharge, as can be highlighted by the large gap between the 80% and 60% SoC curves in Figure 6. The $LiFePO_4$ cell has the opposite characteristics, as can be noted by the large difference between the 40% and 20% SoC curves in Figure 7.

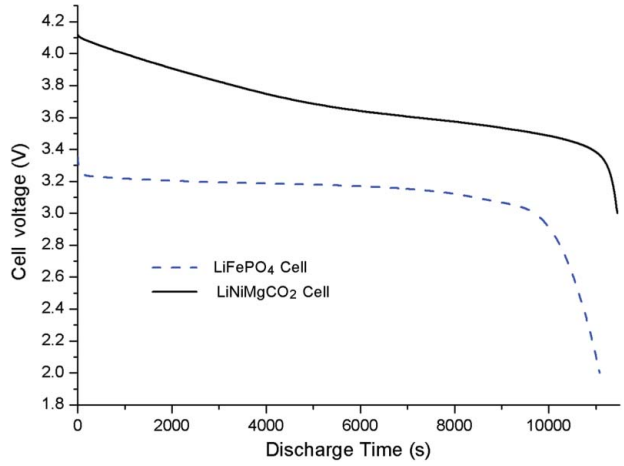


Figure 8. Characteristic discharge curves of $LiNiMgCO_2$ (pouch) and $LiFePO_4$ (cylindrical) cells.

Table 1 is a summary of the results for the discharge tests. The table shows the measured OCV voltage after a 3-hour rest state for each of the test curves. In addition it shows the calculated 3-hour OCV from Equation (3) and the error between the calculated OCV and the measured OCV. These data are supplied for both the pouch cell and the cylindrical cell.

As the test uses constant discharges, the relaxation curve will be positive. This means that Equation (3) had to be used with the addition of the constant $K_v$. The constant $K_v$ was derived from calculating the average difference between the 30-minute OCV measurement and the 3-hour OCV measurement for each of the test curves. Therefore, the chosen $K_v$ values were 0.002 and 0.01 for the pouch and cylindrical cells, respectively. The OCV prediction technique proved to be successful with a maximum error of 3 mV and 5 mV for the pouch and cylindrical cells, respectively. As is derived from alternate tests, the pouch cells have a SoC–OCV relationship of 1% SoC equals 9.9 mV. Therefore the pouch cell resulted in a SoC error of less than 1%. This is a vast improvement on the 5% error recorded by Aylor et al. (1992).

### *3.4. Cell relaxation testing charge state*

The success of the OCV prediction mechanism following a constant current discharge has led to a continuation of research into the relaxation curves following a constant current charge state, and also into a quicker OCV prediction to make the system more practical in real world applications. To conduct the research into the charge relaxation curves, the cell was discharged down to 0% SoC and then charged in 20% steps to 80% SoC as can be seen in Figure 9.

As with the discharge tests in Section 3.3, the tests were conducted at 0.3C, 1C and 3C. The $LiNiMgCO_2$ pouch cell

Table 1. Comparison of measured OCV and calculated OCV after a 3-hour rest period for discharge tests.

| | Pouch cell | | | Cylindrical cell | | |
|---|---|---|---|---|---|---|
| | 180 minute (real) | 180 minute (calc) | Error (mV) | 180 minute (real) | 180 minute (calc) | Error (mV) |
| 0.3C 80% SoC | 3.929 | 3.929 | 0 | 3.328 | 3.332 | 4 |
| 0.3C 60% SoC | 3.759 | 3.759 | 0 | 3.293 | 3.296 | 3 |
| 0.3C 40% SoC | 3.675 | 3.676 | 1 | 3.287 | 3.288 | 1 |
| 0.3C 20% SoC | 3.593 | 3.595 | 2 | 3.21 | 3.212 | 2 |
| 1C 80% SoC | 3.934 | 3.937 | 3 | 3.333 | 3.333 | 0 |
| 1C 60% SoC | 3.766 | 3.766 | 0 | 3.293 | 3.298 | 5 |
| 1C 40% SoC | 3.679 | 3.681 | 3 | 3.289 | 3.29 | 1 |
| 1C 20% SoC | 3.599 | 3.601 | 2 | 3.219 | 3.22 | 1 |
| 3C 80% SoC | 3.932 | 3.933 | 1 | 3.333 | 3.333 | 0 |
| 3C 60% SoC | 3.766 | 3.763 | 3 | 3.294 | 3.298 | 4 |
| 3C 40% SoC | 3.677 | 3.678 | 1 | 3.291 | 3.291 | 0 |
| 3C 20% SoC | 3.601 | 3.601 | 0 | 3.221 | 3.222 | 1 |

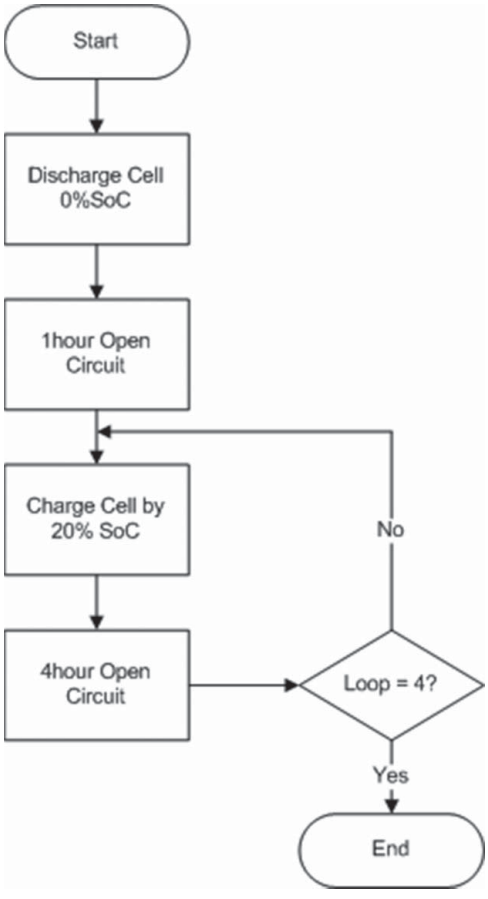


Figure 9. Charge test programme flowchart.

results can be seen in Table 2. Figure 10 shows the four relaxation curves for the 3C charge relaxation test.

The most notable difference between the discharge and charge curves (Figures 6 and 10) is the fact that the charge results in a declining relaxation curve. This is as expected from first principles, as the charge voltage needs to be higher than the cell voltage to reverse the electron flow. Therefore, the voltage falls from the charging voltage to the OCV when the cell charger is removed. The larger voltage difference between 80% and 60% curves in comparison to that of the other curves is expected from the OCV–SoC relationship, as can be seen in Figure 4.

From the relaxation curves in Figure 10 an observation was made that the curve became linear for the $LiNiMgCO_2$ cells after 8 minutes. Therefore, during analysis the voltage measurement taken for the value $V_{tr}$ in Equation (3) was the 8-minute measurement. As the voltage is falling after a charge state, the constant $K_v$ is subtracted from the measurement $V_{tr}$. To ensure that the 8-minute prediction interval was optimum for the type of cell, the relationship between the error and the prediction time was calculated. Figure 11 shows the error vs. relaxation time for the 0.3C charge test at 80%, 60%, 40% and 20% SoC.

Similarly to the relaxation tests in Section 3.3, the constant $K_v$ was derived from the average of the difference between the 8-minute and 180-minute measurements for each of the relaxation curves. Therefore, for the charging relaxation test, the constant $K_v$ was calculated as 0.0087. The following worked example shows the calculation for a relaxation curve following a 0.3C charge at 60% SoC.

$$V_{OC} = V_{tr} - K_v$$

$$V_{OC} = 3.737V - 0.0087$$

$V_{OC} = 3.728V$ is obtained. From the experimental tests conducted,

$V_{real} = 3.729V$ and therefore the error is 0.7 mV, as shown later.

Table 3 provides a comparison of the voltage measurements at the 180-minute interval and the calculated voltage at 180 minutes for all charge relaxation curves. It can be noted that the maximum calculated error for the pouch cells during a charge test was 8.3 mV. As mentioned in Section 3.3, it has been established that for each of the $LiNiMgCO_2$ cells, 9.9 mV of the OCV represents a SoC of

Table 2. Voltage measurements from pouch cell charge relaxation tests.

| Cell test | 0 (minute) | 8 (minute) | 30 (minute) | 60 (minute) | 120 (minute) | 180 (minute) |
|---|---|---|---|---|---|---|
| 0.5C 80% SoC | 3.92 | 3.891 | 3.889 | 3.888 | 3.887 | 3.887 |
| 0.5C 60% SoC | 3.775 | 3.737 | 3.732 | 3.731 | 3.73 | 3.729 |
| 0.5C 40% SoC | 3.702 | 3.671 | 3.668 | 3.667 | 3.666 | 3.665 |
| 0.5C 20% SoC | 3.632 | 3.594 | 3.588 | 3.586 | 3.585 | 3.584 |
| 1C 80% SoC | 3.948 | 3.892 | 3.889 | 3.888 | 3.888 | 3.888 |
| 1C 60% SoC | 3.786 | 3.73 | 3.72 | 3.719 | 3.718 | 3.718 |
| 1C 40% SoC | 3.72 | 3.665 | 3.661 | 3.66 | 3.658 | 3.658 |
| 1C 20% SoC | 3.625 | 3.586 | 3.578 | 3.576 | 3.573 | 3.572 |
| 3C 80% SoC | 4.027 | 3.885 | 3.882 | 3.883 | 3.883 | 3.883 |
| 3C 60% SoC | 3.904 | 3.737 | 3.724 | 3.721 | 3.72 | 3.72 |
| 3C 40% SoC | 3.815 | 3.668 | 3.661 | 3.66 | 3.66 | 3.66 |
| 3C 20% SoC | 3.736 | 3.587 | 3.578 | 3.576 | 3.574 | 3.574 |

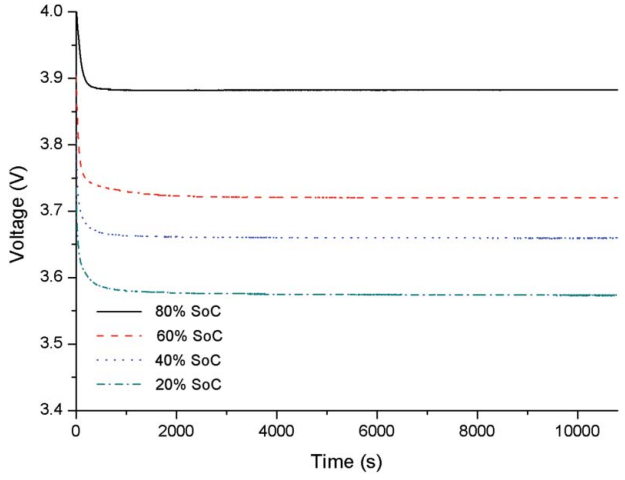


Figure 10. Relaxation curves of lithium pouch cell following a 3C charge.

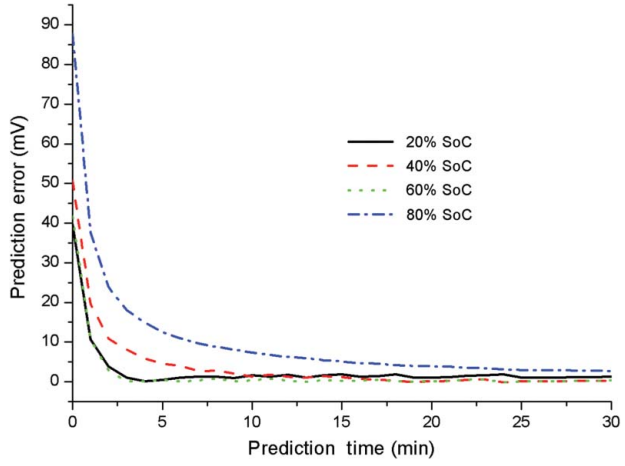


Figure 11. Prediction error vs. relaxation time.

1%. Therefore, a maximum error of just 8.3 mV equals an error of less than 1% SoC at a prediction time of 8 minutes.

This SoC estimation technique also works on the cylindrical $LiFePO_4$ cells, as can be seen by the comparison of the measured and calculated results in Table 5. The same procedure was followed as in the pouch cell tests, and the results of the test can be seen in Table 4.

As Table 5 shows, the charge relaxation tests proved to be effective, with a maximum error of just 11 mV.

Table 3. Calculation results of Equation (3) for pouch cells during a constant current charge test.

| Cell test | 8 minute | 180 minute (real) | 180 minute (calc) | Error (mV) |
|---|---|---|---|---|
| 0.5C 80% SoC | 3.891 | 3.887 | 3.8823 | 4.7 |
| 0.5C 60% SoC | 3.737 | 3.729 | 3.7283 | 0.7 |
| 0.5C 40% SoC | 3.671 | 3.665 | 3.6623 | 2.7 |
| 0.5C 20% SoC | 3.594 | 3.584 | 3.5853 | 1.3 |
| 1C 80% SoC | 3.892 | 3.888 | 3.8833 | 4.7 |
| 1C 60% SoC | 3.73 | 3.718 | 3.7213 | 3.3 |
| 1C 40% SoC | 3.665 | 3.658 | 3.6563 | 1.7 |
| 1C 20% SoC | 3.586 | 3.572 | 3.5773 | 5.3 |
| 3C 80% SoC | 3.885 | 3.883 | 3.8763 | 6.7 |
| 3C 60% SoC | 3.737 | 3.72 | 3.7283 | 8.3 |
| 3C 40% SoC | 3.668 | 3.66 | 3.6593 | 0.7 |
| 3C 20% SoC | 3.587 | 3.574 | 3.5783 | 4.3 |

## 4. Mixed state results and implementation

With the success of the discharge and charge tests, a test plan was conducted to allow the pouch cell to be used in a set of mixed states. This test ensured that the OCV prediction technique could be used in a practical system and not just be reserved for charge or discharge only cycles. The test profile can be seen in Figure 12. A positive current represents that the cell is in a charge state and a negative current represents the discharge state.

A notable feature of the profile in Figure 12 is the long open circuit states (periods of 0A). These periods are where the relaxation voltage was measured, and represent the cell at 80%, 60%, 40% and 20% SoC. The relaxation curves measured during these periods can be seen in Figure 13. The charge/discharge current used for this test was ±10A (0.5C).

Table 4. Voltage measurements from cylindrical cell charge relaxation tests.

| Cell test | 0 minute | 8 minute | 30 minute | 60 minute | 120 minute | 180 minute |
|---|---|---|---|---|---|---|
| 0.5C 80% SoC | 3.468 | 3.344 | 3.333 | 3.332 | 3.331 | 3.331 |
| 0.5C 60% SoC | 3.414 | 3.315 | 3.307 | 3.304 | 3.303 | 3.302 |
| 0.5C 40% SoC | 3.385 | 3.312 | 3.302 | 3.3 | 3.299 | 3.228 |
| 0.5C 20% SoC | 3.326 | 3.247 | 3.324 | 3.232 | 3.23 | 3.228 |
| 1C 80% SoC | 3.409 | 3.341 | 3.334 | 3.332 | 3.332 | 3.331 |
| 1C 60% SoC | 3.373 | 3.313 | 3.308 | 3.305 | 3.304 | 3.301 |
| 1C 40% SoC | 3.351 | 3.309 | 3.304 | 3.302 | 3.3 | 3.299 |
| 1C 20% SoC | 3.289 | 3.244 | 3.237 | 3.233 | 3.231 | 3.23 |
| 3C 80% SoC | 3.394 | 3.339 | 3.337 | 3.336 | 3.332 | 3.332 |
| 3C 60% SoC | 3.357 | 3.314 | 3.309 | 3.307 | 3.305 | 3.304 |
| 3C 40% SoC | 3.342 | 3.307 | 3.306 | 3.304 | 3.302 | 3.3 |
| 3C 20% SoC | 3.279 | 3.242 | 3.24 | 3.237 | 3.235 | 3.234 |

Table 5. Calculation results of Equation (3) for cylindrical cells during a constant current charge test.

| Cell test | 8 minute | 180 minute (real) | 180 minute (calculated) | Error (mV) |
|---|---|---|---|---|
| 3C 80% SoC | 3.344 | 3.331 | 3.331 | 0 |
| 3C 60% SoC | 3.315 | 3.302 | 3.302 | 0 |
| 3C 40% SoC | 3.312 | 3.288 | 3.299 | 11 |
| 3C 20% SoC | 3.247 | 3.228 | 3.234 | 6 |
| 1C 80% SoC | 3.341 | 3.331 | 3.328 | 3 |
| 1C 60% SoC | 3.313 | 3.301 | 3.3 | 1 |
| 1C 40% SoC | 3.309 | 3.299 | 3.296 | 3 |
| 1C 20% SoC | 3.244 | 3.23 | 3.231 | 1 |
| 0.3C 80% SoC | 3.339 | 3.332 | 3.326 | 6 |
| 0.3C 60% SoC | 3.314 | 3.304 | 3.301 | 3 |
| 0.3C 40% SoC | 3.307 | 3.3 | 3.294 | 6 |
| 0.3C 20% SoC | 3.242 | 3.234 | 3.229 | 5 |

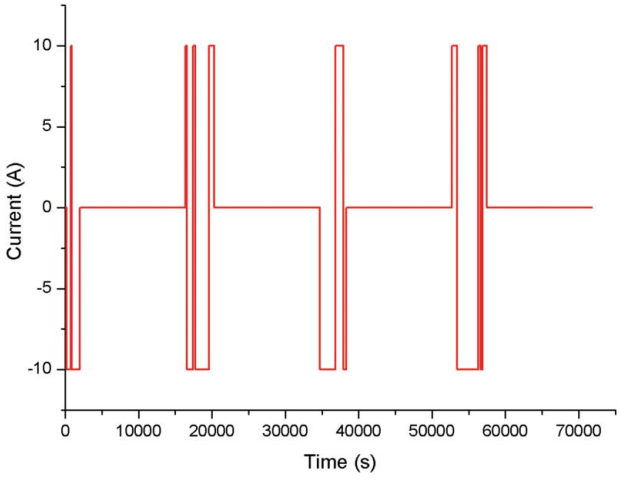


Figure 12. Mixed state test profile.

From both Figures 12 and 13, it can be seen that the profile is split into two relaxation curves following a brief charge state (60% and 20%) and two relaxation curves following a brief discharge state (80% and 40%). This is why two of the relaxation curves fall and two rise.

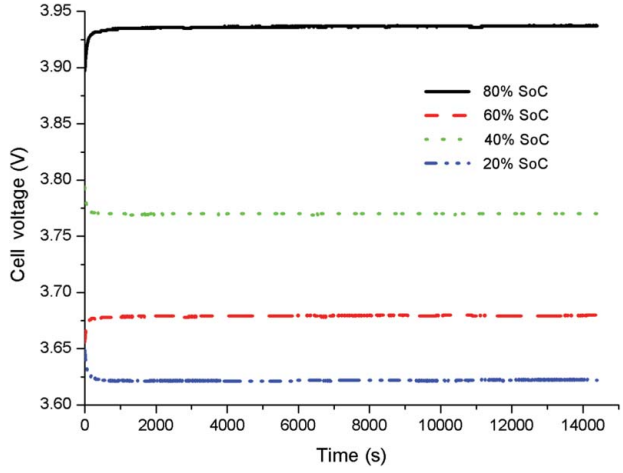


Figure 13. Relaxation curves of lithium pouch cell following a mixed state test profile.

The measurement values from the relaxation curves in Figure 13 are summarised in Table 6.

To test whether Equation (3) (function 2) worked with a mixed state profile, the 8-minute charge and discharge constants ($K_v$) that were calculated for the charge and discharge relaxation tests were used. Therefore the constants used were 0.0083 if the cell is relaxing from a discharge and 0.0087 if the cell is recovering from a charge state. A comparison of the measured and calculated cell voltages at the 180-minute interval is provided in Table 7.

Table 7 shows that the OCV prediction mechanism can be successfully applied to a cell during a mixed state test. This is an important finding as constant charge/discharge curves are rarely seen in practical applications. The maximum error of 13.3 mV shows that the constants ($K_v$) used for the constant discharge and charge tests can be applied to both constant states and mixed states with a SoC error of less than 1.5%.

Figure 14 shows a proposed design for the implementation of the OCV prediction technique into a real world BMS. BMSs currently monitor both cell voltage and the current. This enables the block diagram in Figure 14 to be

Table 6. Relaxation voltage measurements for pouch cells during mixed state test.

| | OCV (V) | | | | | |
|---|---|---|---|---|---|---|
| Cell test | 0 minute | 8 minute | 30 minute | 60 minute | 120 minute | 180 minute |
| 0.5C 80% SoC | 3.897 | 3.903 | 3.935 | 3.936 | 3.937 | 3.937 |
| 0.5C 60% SoC | 3.794 | 3.789 | 3.77 | 3.77 | 3.77 | 3.77 |
| 0.5C 40% SoC | 3.656 | 3.66 | 3.679 | 3.679 | 3.679 | 3.68 |
| 0.5C 20% SoC | 3.649 | 3.644 | 3.621 | 3.621 | 3.622 | 3.622 |

Table 7. Comparison of calculated 3-hour voltage value and measured 3-hour voltage value for mixed state test.

| Cell test | 8 minute | 180 minute (real) | 180 minute (calc) | Error (mV) |
|---|---|---|---|---|
| 0.3C 80% SoC | 3.935 | 3.937 | 3.9433 | 6.3 |
| 0.3C 60% SoC | 3.789 | 3.77 | 3.7803 | 10.3 |
| 0.3C 40% SoC | 3.66 | 3.68 | 3.6683 | 11.7 |
| 0.3C 20% SoC | 3.644 | 3.622 | 3.6353 | 13.3 |

incorporated without major hardware additions. The design can be simply programmed into a small microcontroller.

As aforementioned, the cell voltage and cell current are already known by the BMS as they are both used for alternative functions and safety and are performance based. The cell voltage can easily be stored after an open circuit state of 8 or 30 minutes (OCV measurement block). The start of the open circuit state can be derived from the cell current. The cell current is also monitored by a constant selector. This block works out if the cell has just finished a charge or discharge state, and then chooses the required constant value. For example if the 30-minute measurement was required for higher accuracy, in the case of the pouch cell this would be 0.0026 for the charge state and −0.002 for the discharge state. The $K_v$ constant value would then be summed to the 30-minute OCV measurement to calculate the predicted OCV value after a 3-hour rest state.

Although an OCV prediction time of less than 8 minutes would be practically acceptable in an application such as stand-alone photo-voltaic systems where the battery would not be in constant use, work was conducted to reduce the prediction time to make the system transferable to alternative applications. For this reason, the relaxation curves were studied immediately following the charge or discharge state.

As mentioned in Section 2, a second-order polynomial function has been derived from the results, and takes the following form:

$$\phi = \delta x^2 + \gamma x + \vartheta,$$

where

$$-0.0000467 < \delta < -0.0005$$
$$-0.00865 < \gamma < 0.0242.$$

From the analysis of the polynomials and by the use of simultaneous equations, it can be noted that as the temperature is increased from 25°C to 45°C, the coefficient altered to

$$-0.000046 < \delta < -0.0005$$
$$-0.0085 < \gamma < 0.0235.$$

The polynomial was also calculated for a $LiNiMgCO_2$ pouch cell which has been aged to a capacity of 17.2 Ah from 20.8 Ah. The coefficient values for the aged cell are calculated as follows:

$$-0.000046 < \delta < -0.0005$$
$$-0.0085 < \gamma < 0.0236.$$

However, the coefficients calculated for the temperature change and cell ageing still fall within the range calculated for a new cell at 25°C.

## 5. Performance analysis

The ability to estimate the equilibrated OCV at an interval as little as 8 minutes allows the OCV–SoC method to be used practically in BMSs (Aylor et al., 1992). Furthermore, it is important to note that due to the simplicity of the method described in this work, the equation used in this paper to calculate the equilibrated OCV is so simple that it can be easily implemented into a small microcontroller, as described in the previous section. The results of this paper show that the prediction mechanism works exceptionally well with both charge and discharge states, with a maximum error of 8.3 and 8.25 mV error for the discharge and charge tests, respectively. With a voltage of 9.9 mV resulting in a SoC change of 1%, the simple summation method of function 2 (Equation (3)) is a significant improvement on the ±5% achieved by Aylor et al. (1992). Furthermore, the author of Aylor et al. (1992) used a more complicated mathematical model because of the high errors incurred using Equation (3). The results also show that although the error is very small, there is a difference between the pouch cells and the cylindrical cells, with the cylindrical cells providing a larger error for both the charge and discharge tests. This shows that the constant $K_v$ needs to be calculated for each type of cell prior to cell use. When applied to a mixed

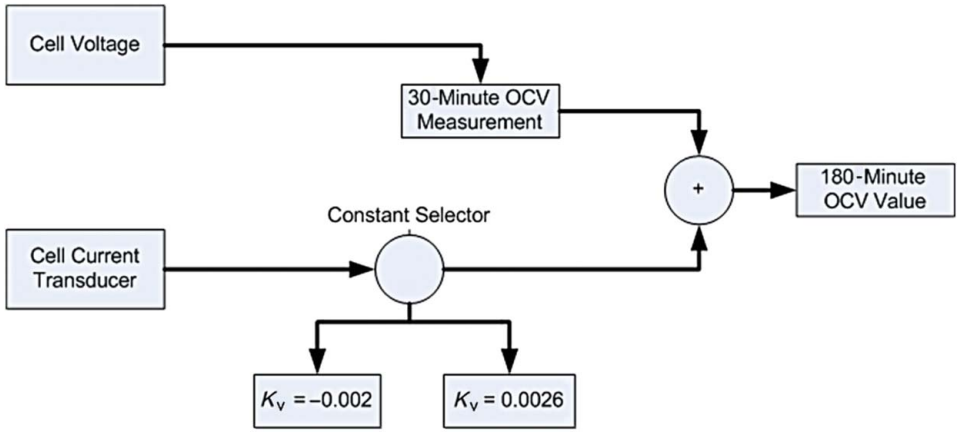


Figure 14. Block diagram of the proposed OCV predictor implementation.

state duty cycle in Section 4, the error was slightly greater but still resulted in a SoC error of less than 1.5%, further proving the function's effectiveness.

A notable point is that although the error is very low at 8 minutes, an OCV prediction at the 30-minute interval as in the original work in Stockley et al. (2013) results in even lower error rates. The maximum error of 8.25 mV for the discharge test and 8.3 mV for the charge test reduces to 3 and 6 mV, respectively. Although the use of the polynomial reduces the possible prediction interval, the error is increased. This is a case for future BMSs in the field of stand-alone PV–lithium hybrid systems to make use of all 3 prediction points. By using all the three methods in a single BMS, the SoC can always be calculated using its most accurate (longest prediction time) value.

## 6. Conclusion

This paper presents a simple but effective methodology to predict the OCV after a small rest period. It used a simple equation to predict the OCV. Previous work had proved that lithium cells had a unique "clone-like" similarity, which is the key for the use of Equation (3), and the high success that occurred during the testing with constant current discharging.

By performing the relaxation tests discussed in Sections 3 and 4, the relaxation curves of several $LiNiMgCO_2$ pouch cells were recorded, so that the equation could be applied following a constant current charge and also during the rest periods of a mixed state duty cycle. By using the OCV at the 8-minute interval, the equilibrated voltage was successfully estimated with a maximum error of just 8.3 mV for the charge tests and 8.25 mV for the mixed state test. The constant current charge tests were also conducted on a set of $LiFePO_4$ cylindrical cells, proving that Equation (3) could be used on a wide variety of lithium cells with a maximum error of 11 mV. In addition to this, possible implementation of this system into a BMS is also described.

## Acknowledgements

The first author would like to acknowledge the financial support from KESS, RUMM Ltd. and the University of South Wales during this research project. The authors would also like to thank the staff of CAPSE for their assistance.

## References

Affanni, A., Bellini, A., Franceschini, G., Guglielmi, P., & Tassoni, C. (2005). Battery choice and management for new-generation electric vehicles. *IEEE Transactions on Industrial Electronics, 52* (5), 1343–1349.

Aylor, J. H., Thieme, A., & Johnson, B. W. (1992). A battery state-of-charge indicator for electric wheelchairs. *IEEE Transactions on Industrial Electronics, 39* (5), 398–409.

Bowkett, M., Thanapalan, K., Stockley, T., Hathway, M., & Williams, J. (2013). *Design and implementation of an optimal battery management system for hybrid electric vehicles*. 19th international conference on automation and computing (ICAC), London, UK (pp. 213–217).

Chiang, Y. H., Sean, W. Y., & Ke, J. C. (2011). Online estimation of internal resistance and open-circuit voltage of lithium-ion batteries in electric vehicles. *Journal of Power Sources, 196* (8), 3921–3932.

Guena, T., & Leblanc, P. (2006). *How depth of discharge affects the cycle life of lithium-metal-polymer batteries*. Telecommunications Energy Conference, INTELEC '06. 28th Annual International, Providence, RI, USA (pp. 1–8).

Hu, X., Li, S., Peng, H., & Sun, F. (2012). Robustness analysis of state-of-charge estimation methods for two types of Li-ion batteries. *Journal of Power Sources, 217*, 209–219.

Li, X., Hui, D., Xu, M., Wang, L., Guo, G., & Zhang, L. (2012). *Integration and energy management of large-scale lithium-ion battery energy storage station*. 2012 15th international conference on electrical machines and systems (ICEMS), Sapporo, Japan (pp. 1–6).

Lu, L., Han, X., Li, J., Hua, J., & Ouyang, M. (2013). A review on the key issues for lithium-ion battery management in electric vehicles. *Journal of Power Sources, 226*, 272–288.

Ng, K. S., Moo, C.-S., Chen, Y.-P., & Hsieh, Y.-C. (2009). Enhanced coulomb counting method for estimating state-of-charge and state-of-health of lithium-ion batteries. *Applied Energy, 86* (9), 1506–1511.

Pei, L., Wang, T., Lu, R., & Zhu, C. (2014). Developement of a voltage relaxation model for rapid open-circuit

voltage prediction in lithium-ion batteries. *Journal of Power Sources, 253*, 412–418.

Pop, V., Bergveld, H. J., Danilov, D., Regiten, P. P. L., & Notten, P. H. L. (2008). Battery Management Systems. In V. Pop, H. J. Bergveld, D. Danilov, P. P. L. Regiten, & P. H. L. Notten, (Eds.), *Methods for measuring and modelling a battery's electro-motive force* (vol. 9, pp. 63–94). Eindhoven, The Netherlands: Springer.

Pop, V., Bergveld, H. J., het Veld, J. H. G. O., Regtien, P. P. L., Danilov, D., & Notten, P. H. L. (2006). Modeling battery behavior for accurate state-of-charge indication. *Journal of the Electrochemical. Society, 153* (11), A2013–A2022.

Roscher, M. A., & Sauer, D. U. (2011). Dynamic electric behavior and open-circuit-voltage modeling of LiFePO4-based lithium ion secondary batteries. *Journal of Power Sources, 196* (1), 331–336.

Salkind, A. J., Fennie, C., Singh, P., Atwater, T., & Reisner, D. E. (1999). Determination of state-of-charge and state-of-health of batteries by fuzzy logic methodology. *Journal of Power Sources, 80* (1–2), 293–300.

Shim, J., & Striebel, K. A. (2003). Characterization of high-power lithium-ion cells during constant current cycling: Part I. Cycle performance and electrochemical diagnostics. *Journal of Power Sources, 122* (2), 188–194.

Sima, A. (2006, October 13). Sony exploding batteries – The chronicles. *Softpedia*. Retrieved from http://news.softpedia.com/news/Sony-Exploding-Batteries-Chronicles-37848.shtml

Stockley, T., Thanapalan, K., Bowkett, M., & Williams, J. (2013). *Development of an OCV prediction mechanism for lithium-ion battery system*. 19th international conference on automation and computing (ICAC), London, UK (pp. 48–53).

Suzuki, I., Shizuki, T., & Nishiyama, K. (2003). *High power and long life lithium-ion battery for backup power sources*. Telecommunications energy conference, 2003. INTELEC '03. The 25th International, Yokohama, Japan (pp. 317–322).

Tremblay, O., & Dessaint, L. A. (2009). Experimental validation of a battery dynamic model for EV applications. *World Electric Vehicle Journal, 3*, 1–10.

Weinert, J. X., Burke, A. F., & Wei, X. (2007). Lead-acid and lithium-ion batteries for the Chinese electric bike market and implications on future technology advancement. *Journal of Power Sources, 172* (2), 938–945.

Weng, C., Sun, J., & Peng, H. (2013, October 21–23). *An open-circuit-voltage model of lithium-ion batteries for effective incremental capacity analysis*. Proceedings of the ASME 2013 Dynamic Systems Control Conference, California, USA.

Zhang, Y., & Harb, J. N. (2013). Performance characteristics of lithium coin cells for use in wireless sensing systems: Transient behavior during pulse discharge. *Journal of Power Sources, 229*, 299–307.